Spin-lattice model of magnetoelectric transitions in RbCoBr$_3$

Tota Nakamura[1] and Yoichi Nishiwaki[2]

[1]*Faculty of Engineering, Shibaura Institute of Technology, Minuma-ku, Saitama 330-8570, Japan*
[2]*Department of Physics, Tokyo Women's Medical University, Shinjuku-ku, Tokyo, 162-8666, Japan*

Extensive Monte-Carlo simulations are performed to analyze a recent neutron-diffraction experiment on a distorted triangular lattice compound RbCoBr$_3$. We consider a spin-lattice model where both spin and lattice are Ising variables. This model explains well successive magnetic and dielectric transitions observed in the experiment. The exchange interaction parameters and the spin-lattice coupling are estimated. It is found that the spin-lattice coupling is important to explain the slow growth of a ferrimagnetic order. The present simulations were made possible by developing a modified Monte-Carlo algorithm, which accelerates slow Monte-Carlo dynamics of quasi-one-dimensional frustrated systems.

I. INTRODUCTION

Frustrated magnets have been attracting much interest for many decades.[1] The ordinary magnetic order is destroyed and the ground state may remain disordered or turn into an exotic state. The ground state of a frustrated system is usually unstable against a small perturbation. The system manages to find a way to relax frustration and change the state. We may design and control material functions using the frustration effects.

The ABX$_3$-type compounds are well-known frustrated magnets. The lattice structure is the stacked triangular lattice. There is frustration when the nearest-neighbor interactions are antiferromagnetic. Successive magnetic phase transitions occur because of the strong frustration when the spins have the Ising anisotropy.[2,3] The low-temperature magnetic structure is the ferrimagnetic state. There exists a partially disordered (PD) phase between the paramagnetic phase and the ferrimagnetic phase. In the PD phase, one of the three sublattices is completely disordered, while the other two sublattices take antiferromagnetic configurations. There is no structural phase transition in most compounds. The system remains fully frustrated down to the lowest temperature.

The KNiCl$_3$-family compounds are exceptional in that they exhibit structural phase transitions.[4–6] We can observe the structural phase transitions by the dielectric measurements because each BX$_3$ chain has a negative charge. These compounds have both magnetic and dielectric characteristics: we call them the magnetodielectric compounds. The magnetic phase transitions and the structural (dielectric) phase transitions usually occur at different temperatures. However, Morishita *et al.*[7,8] found that both transitions occur at the same temperature in RbCoBr$_3$. It is a very rare case among the KNiCl$_3$-family compounds. Magnetic and dielectric measurements[9,10] found that the phase transitions in RbCoBr$_3$ are quite unusual in the following points compared to other compounds:

(i) The dielectric transition temperature of 37 K of RbCoBr$_3$ is very low compared to other compounds for which the transition takes place around the room temperatures. The energy scale of the structural (dielectric) system in RbCoBr$_3$ seems to be suppressed somehow.

(ii) The temperature dependence of the dielectric constant does not exhibit a diverging behavior. This is clearly different from another KNiCl$_3$-family compound RbFeBr$_3$, which exhibits sharp divergence at the transition temperature of 34.4 K.[6]

(iii) The increase in the spontaneous polarization below the dielectric transition temperature is very slow while that of RbFeBr$_3$ is very sharp.

(iv) The magnetic PD phase appears in a very narrow temperature region. The first neutron measurement suggested that it might disappear.[9] A recent improved neutron experiment[11] made it clear that it exists between 31 and 37 K. This is also a clear difference from other compounds such as CsCoBr$_3$ (Ref. 2) and CsCoCl$_3$.[3]

(v) The growth of the ferrimagnetic order is very slow. The neutron count increases linearly with the temperature decrease in the low-temperature phase.

These characteristic behaviors suggest that there is an unknown mechanism of interplay between the magnetic system and the dielectric system in RbCoBr$_3$.

The aim of this paper is to propose a proper theoretical model that *quantitatively* explains the experimental results of RbCoBr$_3$. A well-known theoretical model for the ABX$_3$ compounds is the antiferromagnetic spin system on the stacked triangular lattice.[12–16] However, the ordinary spin model without a coupling to the dielectric system is not sufficient to explain RbCoBr$_3$. The chain-mean-field theory[12] gives the magnitude of the second-nearest-neighbor magnetic interactions on the c plane $|J_2| \simeq 1$ K, which is comparable to that of the nearest-neighbor interactions $|J_1| \simeq 2.5$ K.[8] This is not acceptable from the experimental point of view.

In the present paper, we use the spin-lattice model proposed by Shirahata and Nakamura.[17] This model showed that the PD phase may disappear because of the relaxation of frustration by the lattice distortion; each of the spin system and the lattice system relaxes frustration of the other. A single transition may occur from a paramagnetic and paraelectric phase to the ground-state phase without experiencing the intermediate PD phase. Shirahata and Nakamura also noticed that the cooperation between the spin system and the lattice system works only when the energy scale of the lattice system is comparable to that of the spin system.
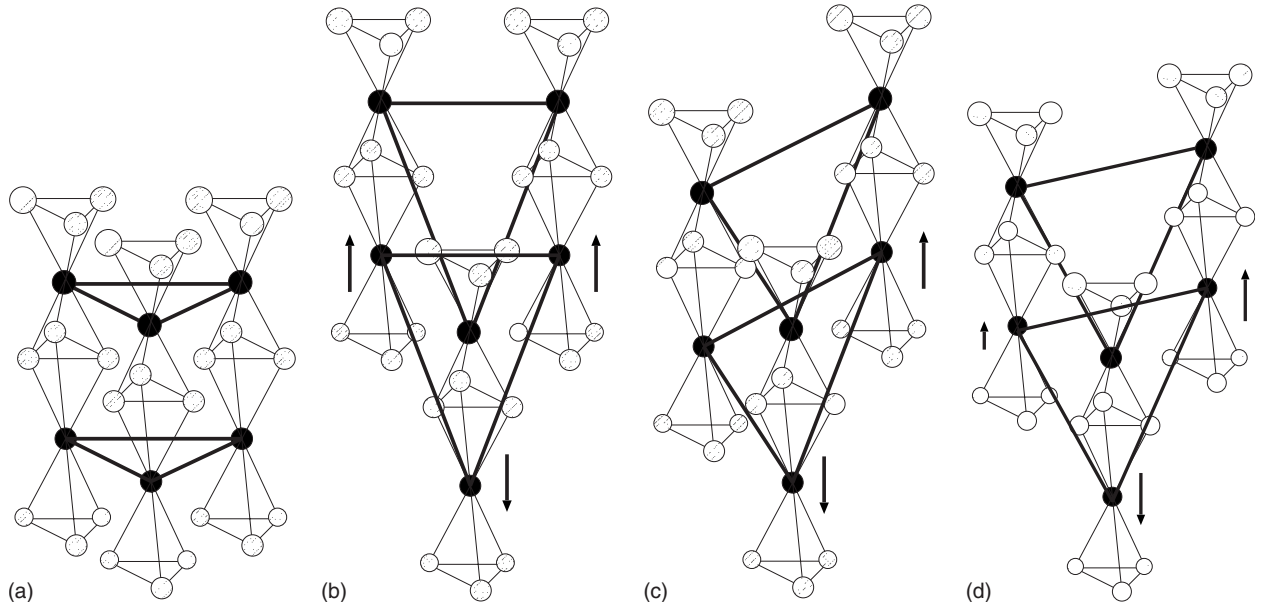
FIG. 1. Typical crystal structures of ABX$_3$-type compounds. A-ions are omitted. Black circles depict magnetic B^{2+} ions and gray circles depict X$^-$ ions. Each arrow depicts the shift direction of a chain. (a) A symmetric structure at high temperatures. The space group is $P6_3/mmc$. (b) A room-temperature KNiCl$_3$ structure. The space group is $P6_3cm$. We call this structure "lattice-Ferri." (c) A low-temperature structure. The space group is $P\bar{3}c1$. We call this structure "lattice-PD." (d) Another low-temperature structure. The space group is $P3c1$. We call this structure a "three-sublattice lattice-Ferri." Each sublattice polarization takes a different value.

In this paper, we refine the above spin-lattice model. We find that a soft lattice system coupled with a spin system explains the interesting material RbCoBr$_3$. We thereby clarify the origin of the characteristic behaviors of this compound. For the purpose, we develop a modified Monte-Carlo (MC) algorithm that eliminates slow MC dynamics in quasi-one-dimensional frustrated spin systems. We have performed extensive MC simulations and determined various physical parameters. We explain our model Hamiltonian in Sec. II. The numerical method is explained in Sec. III and the results are presented in Sec. IV. Discussions are given in Sec. V.

II. THEORETICAL MODEL

A. Structure of ABX$_3$ compounds

The lattice structure of ABX$_3$-type compounds is the stacked triangular lattice. Face-sharing BX$_6$ octahedra run along the c axis forming a BX$_3$ chain. Magnetic B^{2+} ions form an equilateral triangular lattice on the c plane, which causes frustration. Exchange interactions along the BX$_3$ chains J_c are antiferromagnetic. The magnitude of J_c is much larger than that of the nearest-neighbor interactions J_1 on the c plane: $|J_c| \gg |J_1|$. Therefore, this spin system can be considered as a quasi-one-dimensional system with frustration on the c plane.

The typical lattice structure of ABX$_3$-type compounds at high temperatures is shown in Fig. 1(a). The space group is $P6_3/mmc$. Magnetic ions forming an equilateral triangular lattice sit on a level plane. This structure remains down to the lowest temperature in most compounds. In the KNiCl$_3$ family, the structural phase transitions occur as we decrease the temperature. Each BX$_3$ chain shifts upward or downward

keeping the relative distance between the atoms. One of the lattice structures after the structural phase transitions is shown in Fig. 1(b), where two sublattices on the triangular lattice shift upward with the same amount while one sublattice shifts downward. The space group is $P6_3cm$. It is the ferrielectric structure of KNiCl$_3$ observed at room temperatures.[4] We refer to this structure as "lattice-Ferri" or "↑-↑-↓" in this paper. Another possible structure is a configuration with one sublattice shifting upward, one shifting downward, and the third unchanged as shown in Fig. 1(c). The space group is $P\bar{3}c1$. We refer to this structure as "lattice-PD" or "↑-↓-0" in this paper. Nishiwaki and Todoroki[18] discussed the appearance of the three-sublattice ferrielectric state in RbCoBr$_3$ using the mean-field approximation. It is a structure with the ↑-↑-↓ configuration but the amount of displacement in each sublattice is different from the others as shown in Fig. 1(d). The space group is $P3c1$. We refer to this structure as "three-sublattice lattice-Ferri" in order to distinguish from the lattice-Ferri structure of Fig. 1(b), which has the two-sublattice order.

B. Spin-lattice model

We consider a model on the stacked triangular lattice with spin and lattice degrees of freedom.[17] The size in the a and b directions is L, while the size in the c direction is L_c. There are a spin variable S_{ij} and a lattice variable σ_{ij} at each site. Here, the subscript i denotes the position in the c axis, while j denotes the position on the c plane. We define each spin as an Ising variable $S_{ij} = \pm 1/2$ because Co ions have an Ising anisotropy.

The lattice variable σ_{ij} denotes the displacement from the symmetric lattice point along the c axis. We approximate the

displacement with the Ising variable as $\sigma_{ij} = \pm 1/2$; each ion shifts either upward ($\sigma_{ij} = 1/2$) or downward ($\sigma_{ij} = -1/2$). The reason of approximating the present lattice system with the Ising variables is as follows. The symmetric lattice structure with zero displacement as shown in Fig. 1(a) ($P6_3/mmc$) appears at high temperatures. Structural phase transitions occur successively as the temperature decreases. The lattice configuration is the ↑-↓-0 state [Fig. 1(c)] in the intermediate phase and the ↑-↑-↓ state [Fig. 1(b)] in the low-temperature phase. This is analogous to the successive magnetic phase transitions from the paramagnetic phase to the PD phase and to the ferrimagnetic phase in the *Ising* model on the stacked triangular lattice. In the previous paper,[17] we considered a lattice variable taking three states $+1, 0, -1$. Here, we omit a state $\sigma_{ij} = 0$. The $\sigma_{ij} = 0$ state can be represented by a mixture of the $\sigma_{ij} = 1/2$ state and the $\sigma_{ij} = -1/2$ state. A chain shift is the sum of the ion displacements along the chain in the experiment.

The Hamiltonian consists of the lattice part $\mathcal{H}_L$ and the spin part $\mathcal{H}_S$:

$$\mathcal{H} = \mathcal{H}_L + \mathcal{H}_S, \tag{1}$$

where

$$\mathcal{H}_L = -2J_c^L \sum_{i,j} \sigma_{ij}\sigma_{(i+1)j} - 2J_1^L \sum_i \sum_{\langle jk \rangle}^{\text{n.n.}} \sigma_{ij}\sigma_{ik}$$
$$- 2J_2^L \sum_i \sum_{\langle jk \rangle}^{\text{n.n.n.}} \sigma_{ij}\sigma_{ik}, \tag{2}$$

$$\mathcal{H}_S = -2J_c^S \sum_{i,j} S_{ij}S_{(i+1)j} - 2J_1^S \sum_i \sum_{\langle jk \rangle}^{\text{n.n.}} [1 - \Delta(\sigma_{ij} - \sigma_{ik})^2]S_{ij}S_{ik}$$
$$- 2J_2^S \sum_i \sum_{\langle jk \rangle}^{\text{n.n.n.}} [1 - \Delta(\sigma_{ij} - \sigma_{ik})^2]S_{ij}S_{ik}. \tag{3}$$

The lattice part comes from the elastic energy: $(\sigma_{ij} - \sigma_{i'j'})^2$. The spring constant is denoted by $J_{(c,1,2)}^L$, where each of $(c, 1, 2)$ denotes a direction of the interaction: c denotes the c axis, 1 denotes the nearest-neighbor (n.n.) pairs on the c-plane, and 2 denotes the next-nearest-neighbor (n.n.n.) one on the c plane. The sign of the spring constant is determined based on the effect of the exclusion volume effect. It is positive along the c axis: $J_c^L > 0$. An ion pushes the next ion in the same direction. The spring constant for the nearest pairs in the c plane should be negative: $J_1^L < 0$. An ion shifts upward if the neighboring ion shifts downward because ions try to stay away from the neighboring ions. Therefore, there is frustration in the triangular lattice. We choose J_2^L to be positive in order to realize the ↑-↑-↓ state observed experimentally at low temperatures.

The main idea of this paper is to make the spin-spin exchange integrals depend on the lattice variables. We assume that the interaction becomes weak if the exchange path is distorted. Thus, the in-plane exchange interaction becomes $(1-\Delta)$ times weaker if σ_{ij} and σ_{ik} have opposite signs. We
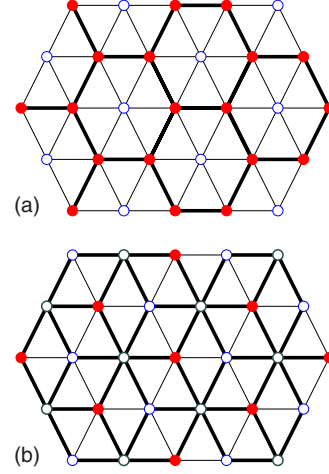

FIG. 2. (Color online) Relaxation of frustration by the lattice distortion. Red (solid) circles depict c chains shifting upward. Blue (gray) circles depict c chains shifting downward. Open (white) circles depict c chains not shifting. Thin (thick) lines depict weak (strong) interactions. (a) When the lattice is deformed to a lattice-Ferri (↑-↑-↓) pattern, the spin-PD state is favored. (b) When the lattice is deformed to a lattice-PD (↑-↓-0) pattern, the spin-Ferri state is favored.

use the same value of Δ for J_1^S and J_2^S for simplicity. The exchange path along the c axis is rigid against the ion shift and hence we assume J_c^S to be unaffected.

We assume that the nearest-neighbor spin-spin interaction is antiferromagnetic ($J_1^S < 0$) and the next-nearest-neighbor interaction is ferromagnetic ($J_2^S > 0$) in order to realize the ferrimagnetic state in the ground state. The interactions along the c axis in the real compound are antiferromagnetic ($J_c^S < 0$).

The lattice part and the spin part of the Hamiltonian have the same form of the antiferromagnetic Ising model on the stacked triangular lattice. They are connected by the Δ term of the form $-4J_{1,2}^S \Delta \sigma_{ij}\sigma_{ik}S_{ij}S_{ik}$. Thus, the present model can be regarded as the Ashkin-Teller model.[19]

Experimental estimates of the exchange integrals were $J_c^S \simeq -62$ K, $J_1^S \simeq -2.5$ K, and $J_2^S \simeq 1$ K.[8] The estimate of J_c^S was obtained from the position of the broad maximum peak of $\chi_\parallel$. We consider it underestimated, which we will discuss in Sec. IV.

C. Relaxation of frustration by lattice distortion

Here, we consider how the ordered magnetic state is favored by the lattice distortion in the present spin-lattice model. When the lattice takes the lattice-Ferri (↑-↑-↓) configuration, the PD state of the spin system is favored magnetically. As shown in Fig. 2(a), the nearest-neighbor interactions between two ↑-shifted sublattices remain strong (depicted in the figure by thick lines), while those between an ↑-shifted sublattice and a ↓-shifted sublattice are weakened by the Δ term. The strong bonds form a honeycomb lattice where the spins are ordered antiferromagnetically. The remaining spins on the ↓-shifted sublattice interact with the spins on the honeycomb lattice through weak bonds. The

molecular field on the ↓-shifted sublattice from the ↑-shifted sublattices vanishes because of the antiferromagnetic ordering on the ↑-shifted sublattices. Then, the spins on the ↓-shifted sublattice may be disordered. We call the PD state of the spin system as "spin-PD" in this paper.

The similar argument is possible when the lattice system takes the lattice-PD (↑-↓-0) state as shown in Fig. 2(b). The ferrimagnetic spin state is favored in this case. The nearest-neighbor interactions between an ↑(↓)-shifted sublattice and a 0-shifted sublattice are weakened by $\Delta/4$, while those between the ↑-shifted sublattice and the ↓-shifted sublattice are weakened by Δ. The antiferromagnetic ordering is realized on the stronger bonds, which is the ferrimagnetic state. We call it in this paper "spin-Ferri." The present mechanism was discussed by Plumer *et al.*,[20] when the lattice distortion is static.

III. MONTE-CARLO METHOD

A. Axial-bond-cluster flip algorithm

We briefly explain our modified Monte-Carlo simulation algorithm. The detail will be reported elsewhere.[21]

The origin of the slow MC dynamics in the quasi-one-dimensional ($|J_c| \gg |J_1|$) Ising system is a very long correlation length along the c axis. It rapidly grows at low temperatures as $\xi_c \sim \exp[|J_c|/T]$. A large magnetic domain along the c axis is not flipped by the standard single-spin-flip algorithm. Koseki and Matsubara[22] introduced a cluster-heat-bath algorithm in order to solve this problem but it costs a long CPU time. The possible size of simulations is restricted to $|J_c/J_1|=10$, $N=36\times36\times360$, and 2×10^6 MC steps.[23]

Here, we solve this problem using the loop algorithm of quantum Monte-Carlo (QMC) simulations.[24] In the QMC simulation, a d-dimensional quantum spin system is mapped to a $(d+1)$-dimensional classical spin system[25] before actual simulations. The additional dimension is called the Trotter direction. Then, the classical spin system for the QMC algorithm can be interpreted as a stacked Ising model. The Trotter direction of the QMC system is now the c axis of the stacked Ising model, and the real-space directions of the QMC system are the c-plane of the stacked Ising model. The loop algorithm of the QMC simulation[24] is to flip a "loop" or an axial aligned-spin cluster along the Trotter direction in the QMC system. Therefore, the algorithm can be readily applied to flip a correlated spin cluster along the c axis of the stacked Ising system.

The size of the cluster is a stochastic variable in each update of the cluster algorithm. Using a proper probability we generate locations of the cluster edges, which are memorized in the computer array. Then, we calculate the sum of molecular fields from other spins to the cluster between two neighboring edges (two arrows in Fig. 3). The cluster is flipped using the heat-bath probability by this molecular field.

We noticed that the required computational procedures and the amount of computer memory are independent of the correlation length ξ_c. We do not need to memorize spin states of all sites. Locations of the cluster edges and the spin state at each chain edge are stored and utilized in the simulation.
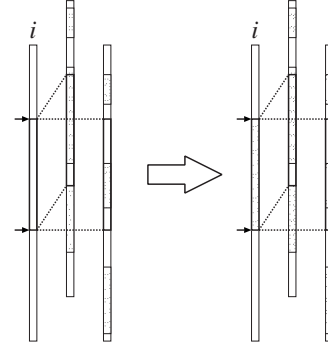

FIG. 3. A schematic of the MC updating procedure. A cluster in an i chain is defined between two edge arrows. It is flipped using the sum of molecular fields from other chains.

The linear size along the c axis L_c is set to ξ_c times larger than L. The system with $L^2 \times \xi_c L$ spins is simulated with an effort of L^3. The modified algorithm becomes exponentially efficient at low temperatures. In this paper, we set $L=104$ for all data. An effective spin number at low temperatures exceeds 10^8. The periodic boundary conditions are imposed on the lattice.

B. Observables

We observe in the present MC simulations the following physical quantities: the sublattice order parameters, one-third-structure factors, one-structure factors, and the uniform magnetic susceptibility. The sublattice order parameters are the sublattice polarization m_η^L and the sublattice magnetization m_η^S, respectively. They are defined as

$$m_\eta^L = \frac{1}{N_{\text{sub}}} \sum_i \sum_{j \in \eta} \sigma_{ij}, \tag{4}$$

$$m_\eta^S = \frac{1}{N_{\text{sub}}} \sum_i (-1)^i \sum_{j \in \eta} S_{ij}, \tag{5}$$

where $\eta = \alpha, \beta, \gamma$ denotes one of three sublattices in the triangular lattice and $N_{\text{sub}} \equiv N/3$.

The following structure factors are defined in order to detect phase transitions and to compare with the neutron experimental data:

$$(f_{1/3}^L)^2 = \frac{1}{8} \left\langle \sum_{\eta = \alpha, \beta, \gamma} (m_\eta^L - m_{\eta+1}^L)^2 \right\rangle, \tag{6}$$

$$(f_{1/3}^S)^2 = \frac{1}{8} \left\langle \sum_{\eta = \alpha, \beta, \gamma} (m_\eta^S - m_{\eta+1}^S)^2 \right\rangle, \tag{7}$$

$$(f_1^L)^2 = \langle (m_\alpha^L + m_\beta^L + m_\gamma^L)^2 \rangle, \tag{8}$$

$$(f_1^S)^2 = \langle (m_\alpha^S + m_\beta^S + m_\gamma^S)^2 \rangle. \tag{9}$$

The one-third-structure factor takes a finite value when the ferrimagnetic state or the PD state is realized. It detects the phase transition between the PD phase and the paramagnetic

phase. The phase transition between the PD phase and the ferrimagnetic phase is detected by f_1.

C. Mean-field-like treatment of MC update

In the present simulation, spin variables and lattice variables are updated separately and alternatively. In the calculation of the heat-bath update probability, we use the following approximation to simplify the simulation. For an update of a spin variable S_{ij}, we calculated the four-body energy $-4J_{1,2}^S \Delta \sigma_{ij}\sigma_{ik}S_{ij}S_{ik}$ by replacing the lattice variable σ_{ij} with a mean value $\bar{\sigma}_j \equiv \Sigma_{i=1}^{Lc} \sigma_{ij}/L_c$, namely, as $-4J_{1,2}^S \Delta(\bar{\sigma}_j\bar{\sigma}_k)S_{ij}S_{ik}$. For an update of a lattice variable σ_{ij}, we replaced the spin variable with a mean value $\bar{S}_j \equiv \Sigma_{i=1}^{Lc} S_{ij}/L_c$, namely, as $-4J_{1,2}^S \Delta(\bar{S}_j\bar{S}_k)\sigma_{ij}\sigma_{ik}$.

This mean-field treatment may be justified by the following argument. In a cluster updating procedure, the sum of the molecular field to a cluster is calculated to estimate the updating probability. Since the cluster size $\sim \exp[|J_c^{S,L}|/T]$ is very large around/below the critical temperature, the mean over a cluster can be approximated by the mean over the whole chain.

The above mean-field treatment possibly influences the critical properties of the phase transitions. Since our main purpose here is to explain the experimental results, most of the simulations are carried out in the off-critical regions. Therefore, we consider that this mean-field treatment does not affect our numerical results in the present paper. The investigations on the critical properties are left for future study.

D. Simulation conditions

The choice of the initial state is important in the present simulation. Since each of the lattice system and the spin system exhibit two successive transitions, we have several possible combinations of ordering patterns as we change the temperature. We therefore used the mixed phase initialization,[26–28] where we prepared several initial spin-lattice states and spatially mixed them. For example, we start the simulation with the following initial state when the temperature is near the spin-PD transition temperature. The lattice system above this temperature takes the lattice-PD ($\uparrow$-$\downarrow$-0) state. Because the spin-PD state favors the lattice-Ferri ($\uparrow$-$\uparrow$-$\downarrow$) state [Fig. 2(a)], they may appear at the same temperature. Therefore, a half of the system is set to the spin-PD state and the lattice-Ferri state, while the other half is set to the spin-paramagnetic state and the lattice-PD state. The former one appears below the transition temperature, while the latter appears above it. We tried other choices of mixed states and verified the equilibration.

The typical number of initialization MC steps was 1000 and that of total MC steps was 10 000. It is sufficient except for the vicinity of the transition temperature. We performed 30 independent MC runs and took the average over these runs.

IV. RESULTS

A. Requirements from the experiments

Experimental findings are listed in the following. They should be reproduced by the simulations.
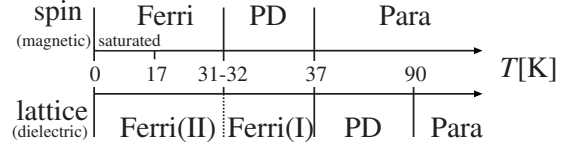

FIG. 4. A phase diagram of RbCoBr$_3$. Solid lines show the known phase-transition temperatures. A broken line at 32 K is another structural transition found in this paper.

(i) The uniform magnetic susceptibility shows a broad peak at $T=100$ K.[10]

(ii) The dielectric constant shows a small anomaly at $T=90$ K (Refs. 7 and 10) where the lattice-PD ($\uparrow$-$\downarrow$-0) state is considered to appear.

(iii) As the temperature decreases from the room temperature, the first magnetic phase transition occurs at $T_{N1}=37$ K. The neutron-scattering data of $(\frac{1}{3}\frac{1}{3}1)$, which corresponds to $(f_{1/3}^S)^2$ of Eq. (7), show a rapid increase below this temperature, while those of (111), which corresponds to $(f_1^S)^2$ of Eq. (9), remains zero. The spin-PD state is considered to appear at this temperature.

(iv) The dielectric constant increases below $T_{N1}=37$ K. The lattice-Ferri ($\uparrow$-$\uparrow$-$\downarrow$) state is considered to appear.[7,10]

(v) The neutron-scattering data of (111) begin to increase at $T_{N2}=31$ K. It is considered as the second magnetic phase transition as the temperature decreases from the room temperature. The temperature dependence of the (111) data is linear with T.[11]

(vi) All the neutron data saturate at $T=17$ K, below which the magnetic order seems to be perfect.[11]

(vii) The dielectric constant also shows an anomaly at 32 K.[10] The temperature is very close to T_{N2}. It is not known whether it is another structural phase transition or not.

The above experimental evidences are summarized in Fig. 4.

Requirement (i) determines the energy scale of J_c^S, requirement (vi) determines J_2^S, requirement (iii) (T_{N1}) determines the ratio J_2^S/J_1^S,[12,21] and requirement (ii) determines the ratio J_2^L/J_1^L. The other parameters are determined by the temperature dependence of the structure factor between 20 and 37 K.
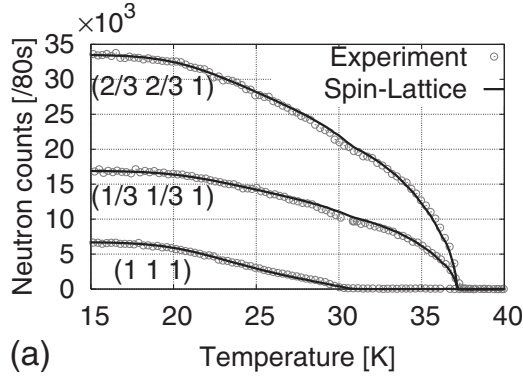
B. Spin-lattice model

Numerical results are shown in Fig. 5. The seven parameters are determined in order to fit the neutron data by visual inspection. The spin parameters are uniquely determined as

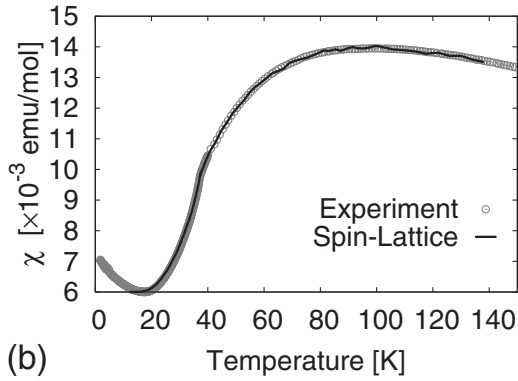$$J_c^S = -97 \text{ K}, \quad J_1^S = -2.4 \text{ K}, \quad J_2^S = 0.14 \text{ K}. \quad (10)$$

Those for the lattice system were not uniquely determined. There are several choices that reproduce the experimental results. We present two choices of the lattice parameters in this paper. Other possible parameter choices range between these two estimates. They are

$$J_c^L = 73 \text{ K}, \quad J_1^L = -49 \text{ K}, \quad J_2^L = 0.38 \text{ K}, \quad \Delta = 0.20,$$
$$(11)$$

and

FIG. 5. Results of the spin-lattice model. The lattice parameters are set to the values in Eq. (11). (a) The MC data of the structure factor are compared with the neutron experimental data (Ref. 11). The MC data of $(f_1^S)^2$ are multiplied to coincide with the experimental data of (111). Those of $(f_{1/3}^S)^2$ are multiplied to coincide with the experimental data of $(\frac{1}{3}\frac{1}{3}1)$ and $(\frac{2}{3}\frac{2}{3}1)$. (b) The MC data of the uniform magnetic susceptibility are compared with the experimental data (Ref. 10). The amplitudes of the simulation data and the constant contribution from the nonmagnetic impurity are determined so that the maximum value and the minimum value agree with the experimental data.

$$J_c^L = 61 \text{ K}, \quad J_1^L = -57 \text{ K}, \quad J_2^L = 0.61 \text{ K}, \quad \Delta = 0.24. \tag{12}$$

Both parameter choices reproduce the neutron data and the susceptibility data fine. Quality of the fitting is the same within the visual inspection. These parameters reproduce the susceptibility data from 20 to 140 K, including a convex change at 37 K. The intermediate phase between 31 and 37 K is identified as the spin-PD phase because the nonequilibrium relaxation data in Fig. 6 exhibits that f_1^S disappears exponentially.

We cannot uniquely determine the lattice parameters because of lack of information that determines J_c^L. In the present lattice system, there is no observable corresponding to the magnetic susceptibility that determines J_c^S. For each choice of J_c^L, we can find J_1^L, J_2^L, and Δ in order to satisfy the experimental data. The ratio J_c^S/J_c^L takes a value from 1.6 to 1.0, which agrees with the previous paper.[17]

We have observed the sublattice magnetization and the sublattice polarization. Figs. 7(a) and 7(b) show the tempera-
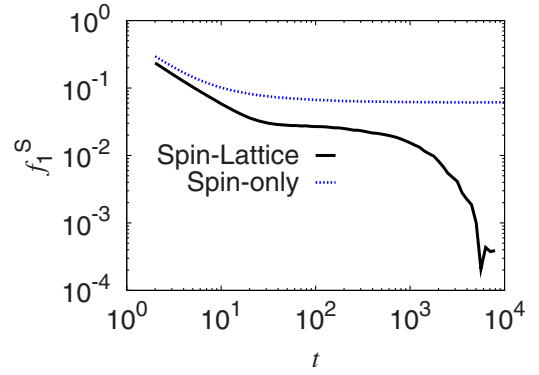

FIG. 6. (Color online) A nonequilibrium relaxation plot of the magnetic structure factor f_1^S when the simulation starts from the ferrimagnetically ordered state. The temperature is 35.5 K, just below $T_{N1}=37$ K. The relaxation function of the spin-only system converges to a finite value, while that of the spin-lattice system decays exponentially. The lattice parameters are those of Eq. (11).

ture dependence of the profiles. As shown in Fig. 7(b), the structural phase transition occurs at $T \simeq 90$ K. Below which the lattice system takes the lattice-PD ($\uparrow$-$\downarrow$-0) state. It reproduces the experimental requirement (ii) of Sec. IV A. The spin system remains paramagnetic in this temperature region.
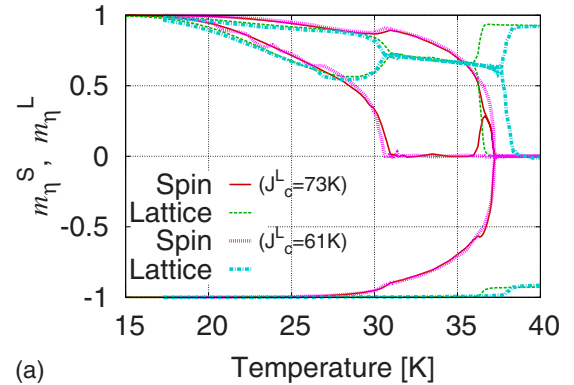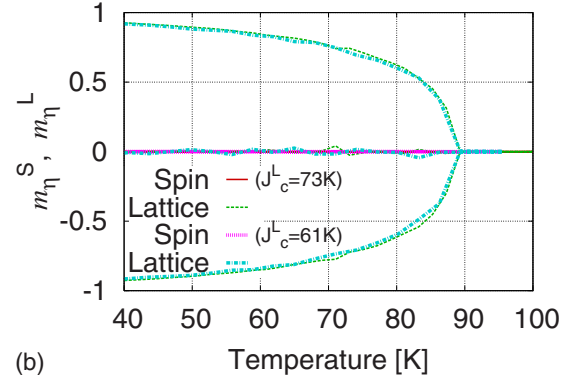
FIG. 7. (Color online) Sublattice profiles of spin variables and lattice variables. The amplitude is normalized to unity when the sublattice order is perfect. Thin (red and green) lines are results of the $J_c^L=73$ K parameter set, while thick (magenta and light blue) lines are results of the $J_c^L=61$ K parameter set, respectively. (a) The temperature ranges from 15 to 40 K, where the corresponding neutron experiments were performed. (b) The high-temperature data.

The spin transition and the lattice transition occur near 37 K [Fig. 7(a)]. They are not always simultaneous. When J_c^L is set to 73 K, the spin transition occurs at 37.2 K, which is slightly higher than the lattice transition temperature of 36.8 K. On the other hand, the lattice transition temperature becomes 38.5 K when J_c^L is set to 61 K, while the spin transition temperature remains the same. The experimental finding of the simultaneous magnetodielectric phase transition at 37 K is an accidental coincidence. The two transitions may occur at slightly different temperatures.

In the case of $J_c^L = 73$ K, a weak ferrimagnetic state appears at 37.2 K. This is because the lattice takes the lattice-PD ($\uparrow$-$\downarrow$-0) state at this temperature, and it favors the spin-Ferri state [Fig. 2(b)]. When the lattice transition occurs at 36.8 K, the spin-Ferri state disappears and the spin-PD state appears because the lattice-Ferri state favors the spin-PD state [Fig. 2(a)]. This is an outcome of the spin-lattice coupling. The situation changes when J_c^L is set to 61 K. The lattice transition occurs at 38.5 K. Since the lattice system takes the lattice-Ferri ($\uparrow$-$\uparrow$-$\downarrow$) state at 37.2 K, the favored spin order is the spin-PD. The weak spin-Ferri state does not appear in this case. This weak ferrimagnetic phase is so narrow that it may not be observed in experiments if it exists.

It is noticed that the spin transition temperature is robust against the change in the lattice parameters. As far as we observed in the MC simulations with several lattice-parameter choices, the spin transition temperature from the paramagnetic phase to the intermediate phase always occurs at 37 K. The spin transition temperature seems to be determined by the spin parameters (10). On the other hand, the lattice system controls the type of the spin order at this temperature.

In the intermediate phase, the amplitudes of two $\uparrow$-shifted sublattice polarization and that of one $\downarrow$-shifted sublattice polarization are different. The former one is not saturated, while the latter is saturated. It is the two-sublattice lattice-Ferri ($\uparrow$-$\uparrow$-$\downarrow$) state [Fig. 1(b)]. An increase in the $\uparrow$-shifted polarization is slow and almost linear with the decreasing temperature.

The low-temperature magnetic transition occurs at 31 K. Below which the ferrimagnetic state appears. Each sublattice magnetization takes a different value. An inversion symmetry between a spin-up sublattice and a spin-down sublattice is broken. It is the three-sublattice ferrimagnetic state, which was predicted to appear by the mean-field approximation.[18] As the temperature decreases, the sublattice magnetizations approach unity and the perfect ferrimagnetic order is realized at temperatures near $T = 17$ K. This saturation temperature depends on J_2^S.

The lattice transition always occurs at the low-temperature magnetic transition temperature. It is the simultaneous spin-lattice phase transition. Above this spin-lattice transition temperature, the lattice system takes the two-sublattice lattice-Ferri state [Fig. 1(b)], which is the ground-state configuration. When the spin-Ferri state appears below the transition temperature, the lattice state is deformed toward the lattice-PD ($\uparrow$-$\downarrow$-0) state because the spin-Ferri state favors the lattice-PD state. A combination of the partial lattice-Ferri state and the partial lattice-PD state yields the
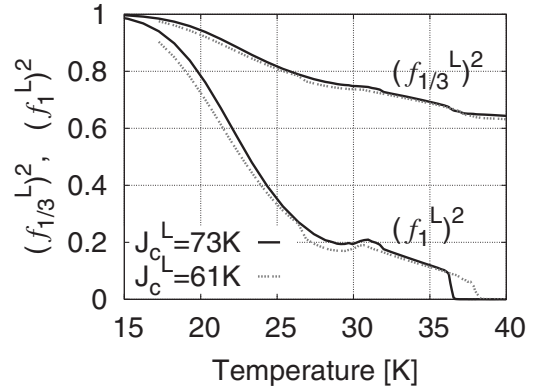

FIG. 8. The structure factor data of the lattice system. The data of $(f_1^L)^2$ are multiplied by 9.

three-sublattice lattice-Ferri state [Fig. 1(d)]. The space group changes from $P\bar{3}c1$ to $P3c1$. It is a clear evidence for a strong correlation between the spin system and the lattice system. The lattice system alone cannot make this structural phase transition because the lattice system is in the ground-state phase above the transition temperature. Therefore, this may be the spin-lattice transition driven by the spin degrees of freedom.

Figure 8 shows the MC results of the structure factor of the lattice system. The $f_{1/3}$-structure factor shows small anomalies at 37 and 31 K. The temperature dependence between 37 and 31 K is slow and almost linear with T. The f_1-structure factor data qualitatively agree with the experimental results of the spontaneous polarization.[10] The data show a decrease below 31 K because the lattice-Ferri state is deformed toward the lattice-PD state by the ferrimagnetic transition. In a real experiment,[10] the spontaneous polarization shows a minimum at 23 K, while the minimum occurs at 28 K in the present simulation.
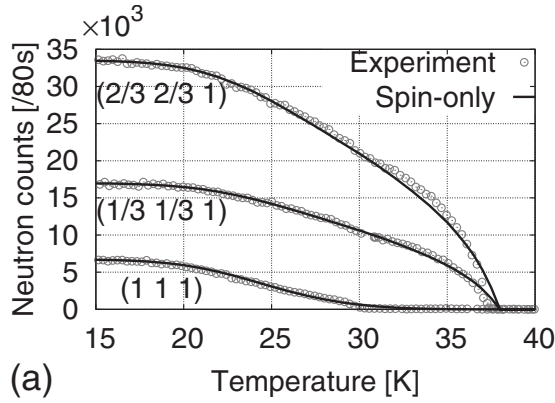
C. Spin-only model

We show that the spin-only system cannot explain all the experimental data. The three parameters J_c^S, J_1^S, and J_2^S are determined in order to fit the neutron experimental data fine by visual inspection. Figure 9 shows the result. The estimates are

$$J_c^S = -77 \text{ K}, \quad J_1^S = -3.8 \text{ K}, \quad J_2^S = 0.58 \text{ K}.$$

Agreement with the neutron data is good, while the susceptibility data disagree with the experiment significantly. If we choose estimates that fit the susceptibility data, the neutron data disagree in turn. We cannot find estimates that satisfy both experimental data at the same time.

The MC data of the structure factor of (111) take very small but finite values between 31 and 37 K as shown in Fig. 6. It suggests that the ferrimagnetic order is finite and the intermediate spin-PD phase disappears. The direct transition from the paramagnetic phase to the ferrimagnetic phase is an outcome of a rather large estimate of J_2^S.

The spin-only model does not consider the dielectric characteristics of RbCoBr$_3$. We cannot explain the successive

(a)
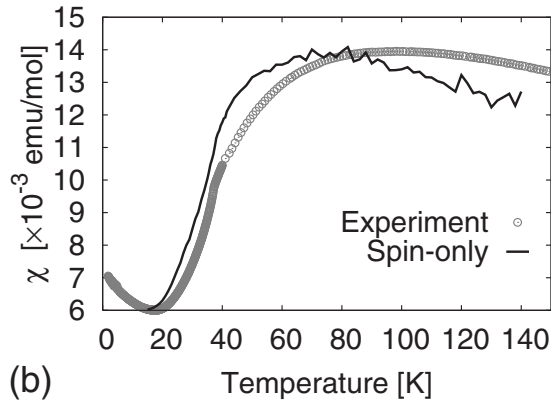
(b)

FIG. 9. Results of the spin-only model. (a) The MC data of the structure factor are compared with the neutron experimental data (Ref. 11). The MC data of $(f_1^S)^2$ are multiplied to coincide with the experimental data of (111). Those of $(f_{1/3}^S)^2$ are multiplied to coincide with the experimental data of $(\frac{1}{3}\frac{1}{3}1)$ and $(\frac{2}{3}\frac{2}{3}1)$. (b) The MC data of the uniform magnetic susceptibility are compared with the experimental data (Ref. 10). The amplitudes of the simulation data and the constant contribution from the nonmagnetic impurity are determined so that the maximum value and the minimum value agree with the experimental data.

structural phase transitions by this model. Using three parameters J_c^S, J_1^S, and J_2^S we only reproduce either the neutron experimental data or the magnetic-susceptibility data. On the other hand, the spin-lattice model explains quantitatively both dielectric and magnetic properties using seven parameters. It suggests that the interplay between the spin system and the lattice system is essential in this compound.
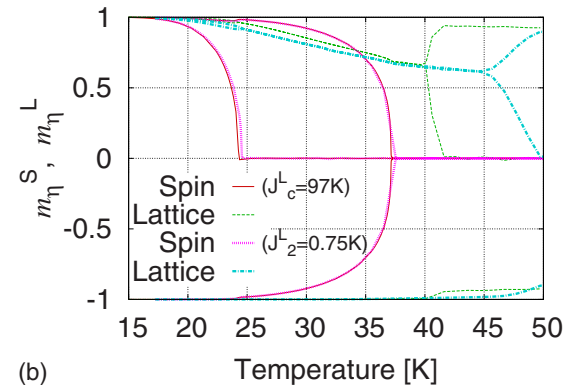
D. Perturbations

We consider perturbation effects to the present model. It is intended to see how robust the characteristic behaviors of RbCoBr$_3$ are against perturbations as well as to propose further experimental investigations. Here, we consider three perturbations. The former two perturbations couple with the lattice system, while the last one changes the spin-lattice coupling parameter.

First, a lattice interaction parameter is changed in order to make the lattice system hard. It corresponds to a pressure effect. We increase the interaction (spring constant) along the
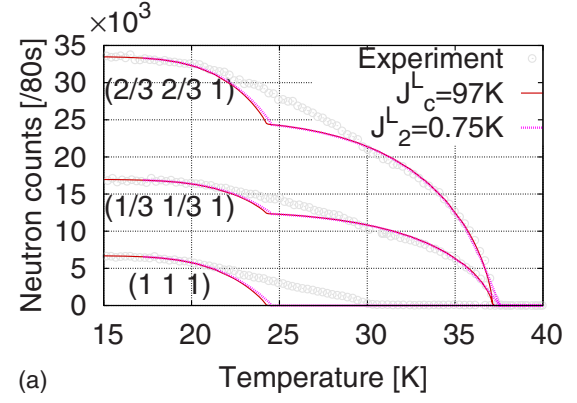
(a)

(b)

FIG. 10. (Color online) Perturbations on exchange interactions. In one case, we increased J_c^L from 73 to 97 K (thin; red and green). In the other case, we increased J_2^L from 0.38 to 0.75 K (thick; magenta and light blue). The other parameters are the same as in Eq. (11). (a) Neutron data of RbCoBr$_3$ are compared with the MC data of the structure factor in the perturbed cases. The MC data are multiplied so that the saturation value coincides with the experimental data at 17 K. (b) Sublattice profiles of the spin and the lattice variables.

c axis J_c^L from 73 to 97 K, while the other parameters remain the same as in Eq. (11). Figure 10 shows the results. The lattice transition to the two-sublattice ↑-↑-↓ state occurs at 40 K [thin green lines in Fig. 10(b)], while it occurs at 37.2 K [thin green line in Fig. 7(a)] in the unperturbed case. The magnetic transition occurs at 37.1 K [red and magenta lines in Fig. 10(b)] and the PD state appears. This magnetic transition temperature is robust against the lattice perturbation. The PD phase continues to the lower temperature and the ferrimagnetic transition occurs at 24 K. We observe the small bifurcation of the lattice profiles at this temperature. The two-sublattice lattice-Ferri state is deformed very weakly to the three-sublattice lattice-Ferri state. The simultaneous spin-lattice transition also occurs in the perturbed system. The PD phase becomes wider as in the typical ABX$_3$ compounds. Another clear difference from the original parameter set is that the (111) structure factor is convex when it appears at 24 K, while the original one is linear.

Second, we changed J_2^L from 0.38 to 0.75 K, while the other parameters remain the same as in Eq. (11). This perturbation favors the lattice-Ferri (↑-↑-↓) state. It may correspond to applying the electric field to this compound. The results of the spin system are the same as the case where we
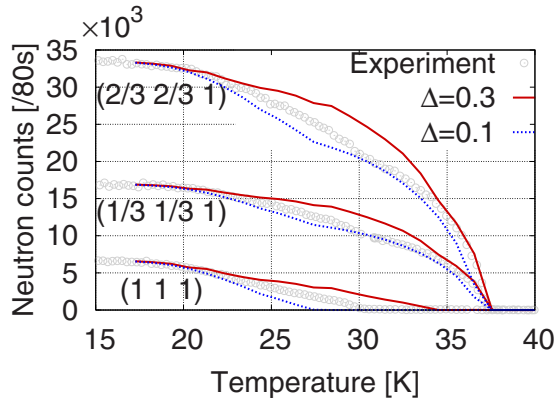
FIG. 11. (Color online) Neutron data of RbCoBr$_3$ are compared with the MC data of the structure factor when Δ is set to 0.1 and 0.3. The other parameters are the same as in Eq. (11). The MC data are multiplied so that the saturation value coincides with the experimental data at 17 K.

changed J_c^L. As shown in the figures, both perturbations produce the same temperature dependences of the spin profiles. On the other hand, the lattice profiles are different. The lattice ↑-↑-↓ transition occurs at 45 K [thick light-blue lines in Fig. 10(b)], while it occurs at 40 K in the J_c^L perturbation. Experiments under the electric field or high pressures may detect these changes.

The last perturbation changes the spin-lattice coupling parameter. We set $\Delta=0.1$ and 0.3 while the other parameters are unchanged from Eq. (11). Figure 11 shows the results of the structure factor compared to the neutron experimental data. The PD transition temperature and the saturation temperature are robust against this perturbation. On the other hand, the ferrimagnetic transition temperature depends on Δ, which is observed by the change in slope of the (111) data. As we increase Δ, the ferrimagnetic transition temperature increases. The spin-lattice coupling relaxes frustration and stabilizes the ferrimagnetic state.

Comparing the above with the results of the original parameters (Figs. 5 and 7) we notice that there are several spin-lattice effects. The ferrimagnetic state appears at higher temperatures because of the relaxation of frustration. The (111) structure factor linearly depends on the temperature. There appears a three-sublattice ↑-↑-↓ state. These characteristic behaviors in RbCoBr$_3$ are fragile and disappear when the spin-lattice coupling changes. Control of the lattice system by the electric field or the pressure may produce a new effect to the spin system.

V. DISCUSSION

The successive phase transitions of RbCoBr$_3$ are well explained by the spin-lattice model introduced in this paper. Numerical data of our Monte-Carlo simulations quantitatively agree with the experimental results. The spin-lattice coupling is found to be essential in this system. It produces nontrivial behaviors of RbCoBr$_3$ different from other typical ABX$_3$ compounds. The present analysis was enabled by the modified cluster flip algorithm, which eliminates the slow

MC dynamics in the quasi-one-dimensional frustrated spin system.

The magnetodielectric transition at 37 K is not always simultaneous. It is a coincidence that the spin transition and the lattice transition occur at the close temperatures in RbCoBr$_3$. They may differ if the interaction parameters are different. The spin transition temperature is possibly determined independently from the lattice system. The spin-lattice coupling only determines what type of the spin order is realized below this transition temperature.

On the other hand, the magnetodielectric transition at 31 K is always simultaneous. It is the spin-driven lattice transition. The lattice symmetry changes in order to realize the ferrimagnetic state. Therefore, the anomaly of the spontaneous polarization observed experimentally[10] at 32 K is considered as an indication of another structural transition, where the space group changes from $P\bar{3}c1$ to $P3c1$. Further experiments to ensure this theoretical prediction are expected. An anomaly at 9 K observed experimentally has not been identified within the present spin-lattice model.

The criticality of the phase transitions is an interesting future problem. The linear temperature dependence of the (111) structure factor below 31 K in Fig. 5(a) may be an indication of the mean-field universality $\beta=1/2$. Although the interaction range is limited to the second-nearest neighbor, the spin-lattice coupling effectively makes it long range because of the large correlation lengths of both spin variables and lattice variables. This mean-field criticality is supported by a model proposed recently by Miyashita *et al.*[29] Their model for a magnetic phase transition in spin-crossover materials is similar to our spin-lattice model. In their model, the spin takes either a high-spin state or a low-spin state. The volume of a magnetic ion depends on the spin state, which produces an effective spin-lattice coupling. They observed the mean-field universality by the detailed scaling analysis on the model system. If the mean-field universality appears in RbCoBr$_3$, it may be observed in other magnetodielectric compounds, e.g., RFe$_2$O$_4$.[30,31]

It should be commented that our mean-field-like treatment of the MC updating may have affected the critical phenomenon. This treatment averages the lattice variables along the chain. It may produce effective long-range spin-spin correlations along the chain.

In the present model, the lattice parameters have not been determined uniquely. The lattice model is simple, taking only the elastic energy into account. Our assumption of the spin-lattice coupling only models the deformation of the lattice system as an influence to the spin system. Some modifications to the model may be necessary when we discuss the magnetic-dielectric cross correlation under an electric field and a magnetic field.

[1] For example, articles in Proceedings of the International Conference on Highly Frustrated Magnetism, Osaka, Japan, 15–19 August 2006 [J. Phys.: Condens. Matter 19 (14) (2007)].

[2] W. B. Yelon, D. E. Cox, and M. Eibschütz, Phys. Rev. B **12**, 5007 (1975).

[3] M. Mekata and K. Adachi, J. Phys. Soc. Jpn. **44**, 806 (1978).

[4] D. Visser, G. C. Verschoor, and D. J. W. Ijdo, Acta Crystallogr., Sect. B: Struct. Crystallogr. Cryst. Chem. **36**, 28 (1980).

[5] K. Adachi, K. Takeda, F. Matsubara, M. Mekata, and T. Haseda, J. Phys. Soc. Jpn. **52**, 2202 (1983).

[6] T. Mitsui, K. Michida, T. Kato, and K. Iio, J. Phys. Soc. Jpn. **63**, 839 (1994).

[7] K. Morishita, T. Kato, K. Iio, T. Mitsui, M. Nasui, T. Tojo, and T. Atake, Ferroelectrics **238**, 105 (2000).

[8] K. Morishita, K. Iio, T. Mitsui, and T. Kato, J. Magn. Magn. Mater. **226-230**, 579 (2001).

[9] Y. Nishiwaki, T. Kato, Y. Oohara, and K. Iio, J. Phys. Soc. Jpn. **73**, 2841 (2004).

[10] Y. Nishiwaki, H. Imamura, T. Mitsui, H. Tanaka, and K. Iio, J. Phys. Soc. Jpn. **75**, 094702 (2006).

[11] Y. Nishiwaki, A. Oosawa, T. Nakamura, K. Kakurai, N. Todoroki, N. Igawa, Y. Ishii, and T. Kato, J. Phys. Soc. Jpn. **77**, 104703 (2008).

[12] H. Shiba, Prog. Theor. Phys. **64**, 466 (1980).

[13] F. Matsubara and S. Inawashiro, J. Phys. Soc. Jpn. **53**, 4373 (1984).

[14] T. Kurata and H. Kawamura, J. Phys. Soc. Jpn. **64**, 232 (1995).

[15] O. Koseki and F. Matsubara, J. Phys. Soc. Jpn. **69**, 1202 (2000).

[16] N. Todoroki and S. Miyashita, J. Phys. Soc. Jpn. **73**, 412 (2004).

[17] T. Shirahata and T. Nakamura, J. Phys. Soc. Jpn. **73**, 254 (2004).

[18] Y. Nishiwaki and N. Todoroki, J. Phys. Soc. Jpn. **75**, 024708 (2006).

[19] J. Ashkin and E. Teller, Phys. Rev. **64**, 178 (1943); C. Fan, Phys. Lett. **39A**, 136 (1972).

[20] M. L. Plumer, A. Caillé, and H. Kawamura, Phys. Rev. B **44**, 4461 (1991).

[21] T. Nakamura, arXiv:0809.2969 (unpublished).

[22] O. Koseki and F. Matsubara, J. Phys. Soc. Jpn. **66**, 322 (1997); F. Matsubara, A. Sato, O. Koseki, and T. Shirakura, Phys. Rev. Lett. **78**, 3237 (1997).

[23] E. Meloche and M. L. Plumer, Phys. Rev. B **76**, 174430 (2007).

[24] T. Nakamura and Y. Ito, J. Phys. Soc. Jpn. **72**, 2405 (2003).

[25] *Quantum Monte Carlo Methods in Condensed Matter Physics*, edited by M. Suzuki (World Scientific, Singapore, 1994).

[26] C. Rebbi, Phys. Rev. D **21**, 3350 (1980).

[27] F. Fucito and A. Vulpiani, Phys. Lett. **89A**, 33 (1982).

[28] Y. Ozeki, K. Kasono, N. Ito, and S. Miyashita, Physica A **321**, 271 (2003).

[29] S. Miyashita, Y. Konishi, M. Nishino, H. Tokoro, and P. A. Rikvold, Phys. Rev. B **77**, 014105 (2008).

[30] N. Ikeda, H. Ohsumi, K. Ohwada, K. Ishii, T. Inami, K. Kakurai, Y. Murakami, K. Yoshii, S. Mori, Y. Horibe, and H. Kitô, Nature (London) **436**, 1136 (2005).

[31] A. Nagano, M. Naka, J. Nasu, and S. Ishihara, Phys. Rev. Lett. **99**, 217202 (2007).